Molecular Ferroelectrics

DOI: 10.1002/anie.201400348

A Molecular Ferroelectric Thin Film of Imidazolium Perchlorate That Shows Superior Electromechanical Coupling**

Yi Zhang, Yuanming Liu, Heng-Yun Ye, Da-Wei Fu, Wenxiu Gao, He Ma, Zhiguo Liu, Yunya Liu, Wen Zhang, Jiangyu Li, Guo-Liang Yuan, and Ren-Gen Xiong**

Abstract: *Molecular ferroelectric thin films are highly desirable for their easy and environmentally friendly processing, light weight, and mechanical flexibility. A thin film of imidazolium perchlorate processed from aqueous solution is an excellent molecular ferroelectric with high spontaneous polarization, high Curie temperature, low coercivity, and superior electromechanical coupling. These attributes make it a molecular alternative to perovskite ferroelectric films in sensing, actuation, data storage, electro-optics, and molecular/flexible electronics.*

Ferroelectrics are electroactive materials with versatile properties. They possess spontaneous polarization that is sensitive to temperature change, electric field, and mechanical stress,[1] making them attractive for thermal imaging, data storage, mechanical actuation, and energy harvesting.[2] They also exhibit nonlinear dielectric and optic effects that can be tuned by an electric field,[3] and thus can be used to manipulate electromagnetic waves.[4] While applications of ferroelectrics are currently dominated by inorganic perovskite materials, such as lead zirconate titanate (PZT) and barium titanate (BTO),[5] in the last a few years significant breakthroughs have also been witnessed in molecular ferroelectrics that are lightweight,[6] mechanically flexible, and environmentally friendly, with their ferroelectric properties approaching those of perovskites.[7] For example, croconic acid was shown to possess a high spontaneous polarization of around 23 $\mu C\,cm^{-2}$,[8] which is comparable to that of BTO, while diisopropylammonium bromide (DIPAB) was found to have a high ferroelectric phase transition temperature of 426 K, exceeding that of BTO as well as new ferroelectric physics,[9] such as charge-transfer along $\pi\cdots\pi$-stacked supramolecular networks of electron donors and acceptors leading to spontaneous polarization.[10] Despite these exciting advances towards molecular ferroelectric crystals, molecular ferroelectric thin films have rarely been reported,[11] and their ferroelectric properties are far inferior to those of perovskite films,[12] hindering their applications in microelectromechanical systems (MEMS), ferroelectric random-access memory (FeRAM), and even as solar-cell sensitizers,[13] wherein miniaturization and integration are essential. Herein, we show that a molecular ferroelectric thin film of imidazolium perchlorate (Im-ClO_4) processed from aqueous solution exhibits superior electromechanical coupling exceeding that of PZT films, making them an attractive lead-free alternative for a variety of applications.

During our systematic searching for molecular ferroelectrics,[14] imidazolium perchlorate (Im-ClO_4),[15] a trigonal crystal similar to $LiNbO_3$, caught our attention owing to its high melting temperature, high ferroelectric phase transition temperature (Supporting Information, Figure S1). The structure analysis (Supporting Information, Figures S2, S3) and second harmonic generation (SHG) (Figure 1 A) measurement reveal that Im-ClO_4 is polar below $T_c = 373.6$ K, which was confirmed by our pyroelectric measurement. As shown in Figure 1 A, spontaneous polarization integrated from pyroelectric current perpendicular to the $[10\bar{2}]$ plane starts to appear at 373.2 K, which is consistent with the transition temperature of 373.6 K obtained from DSC, and the spontaneous polarization reaches 9.3 $\mu C\,cm^{-2}$ at 310 K, one of the highest among molecular ferroelectrics. To verify the ferroelectricity of the crystal, both real and imaginary parts of the dielectric constant as a function of bias electric field were measured, which show characteristic butterfly loops, indicative of polarization switching (Figure 1 B). This was further confirmed by polarization hysteresis recorded using Sawyer–Tower circuit (Figure 1 C). The measured polarization is around 7.5 $\mu C\,cm^{-2}$, consistent with pyroelectric measurement. More interestingly, the piezoelectric coefficient d_{33} reaches 41 $pC\,N^{-1}$, as shown in Figure 1 D, one of the highest in molecular ferroelectrics. For example, the piezoelectric coefficient d_{33} of triglycine sulfate (TGS), PVDF, and $LiNbO_3$

[*] Dr. Y. Zhang,[+] Dr. H.-Y. Ye, Dr. D.-W. Fu, Prof. W. Zhang, Prof. R.-G. Xiong
Ordered Matter Science Research Center
Southeast University, Nanjing 211189 (P. R. China)
E-mail: xiongrg@seu.edu.cn
Prof. Y. M. Liu,[+] Prof. J. Y. Li
Department of Mechanical Engineering
University of Washington, Seattle, WA 98195 (USA)
W. X. Gao, H. Ma, Prof. G. L. Yuan
School of Materials Science and Engineering
Nanjing University of Science and Technology
Nanjing 210094 (P.R. China)
E-mail: yuanguoliang@njust.edu.cn
Prof. Z. G. Liu
Department of Materials Science and Engineering
Nanjing University, Nanjing 210093 (P.R. China)
Prof. Y. Y. Liu
Faculty of Materials, Optoelectronics and Physics
Key Laboratory of Low Dimensional Materials and Application Technology of Ministry of Education
Xiangtan University, Hunan 411105 (China)
[+] These authors contributed equally to this work.

[**] This work was supported by the 973 project (2014CB932103) and the National Natural Science Foundation of China 21290172, 11134004, 21371032, and USA NSF CMMI 1100339.
Supporting information for this article is available on the WWW under http://dx.doi.org/10.1002/anie.201400348.

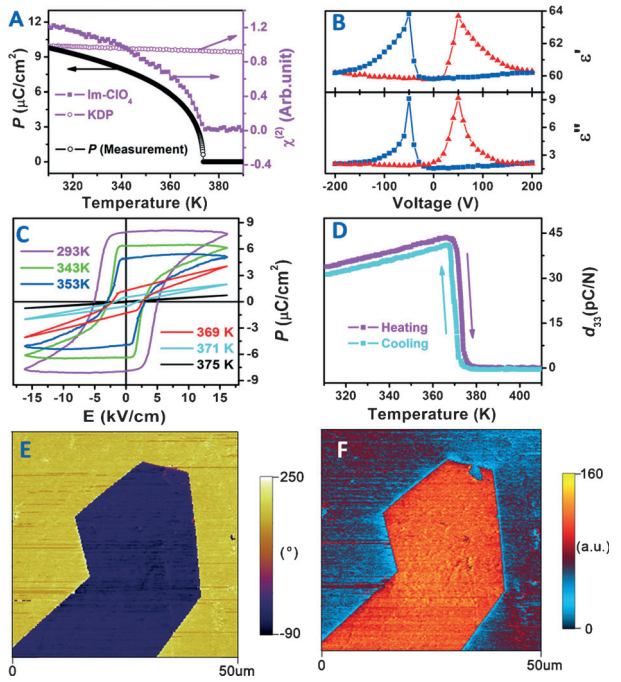

Figure 1. The ferroelectricity and related properties of Im-ClO_4. A) SHG signal and spontaneous polarization as functions of temperature. The SHG signal of KDP was recorded for comparison; B) Bias field dependence of the dielectric constant with butterfly loops showing polarization switching or domain switching; C) Polarization hysteresis loops at different temperatures; D) Temperature-dependent piezoelectric constant; E) PFM phase mapping of the (10$\bar{2}$) plane of the single crystal; and F) PFM amplitude mapping the (10$\bar{2}$) plane of the single crystal.

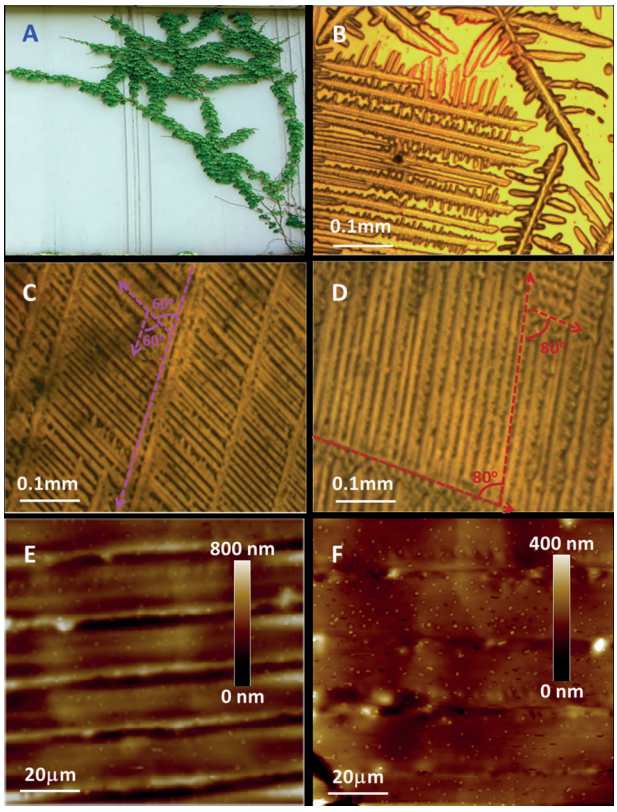

Figure 2. Morphologies of the dendritic crystal growth of Im-ClO_4 on a millimeter scale on Si/SiO2/Ti/Pt or quartz substrate. A) An Ivy vine climbing from a root, to which a dendritic crystal growth from a crystal nucleus is similar; B) The early stage of the dendritic crystal growth like a vine climbing a wall; C), D) Optical images of dendritic crystals with 60° and 80° between stem and branches; E), F) AFM images of the last stage of the dendritic crystal growth.

are 35, 31, and 8 pCN^{-1}, respectively.[16] Moreover, its piezoresponse force microscopy (PFM) mappings show characteristic hexagonal phase (Figure 1E) and amplitude (Figure 1F) images as expected from a trigonal crystal, similar to those observed in $LiNbO_3$.

The excellent ferroelectricity of the Im-ClO_4 crystal motivated us to process a thin film of Im-ClO_4 for easier miniaturization and integration, which we succeeded using the simple and inexpensive spin-coating approach. The procedure in preparation of the film includes the deposition of the 2–5 layers of thin film of Im-ClO_4 on an amorphous Si/SiO_2/Ti/Pt or quartz substrate by the spin-coating method, and then dendrite crystal growth on this substrate plate (see the Experimental Section). Millimeter-scale Im-ClO_4 dendritic crystals were neatly grown. During dendrites growth in a saturated solution with the solubility of about 60%, the stems grow in several preferred directions continuously like a vine climbing a wall (Figure 2A,B).[17] The width and the thickness of stem and branches do not obviously change at the early stage of the dendrtic crystal growth. There are two main patterns of dendritic crystals where the angle between a stem and its branches is 60° (Figure 2C) and 80° (Figure 2D). The stem and branches with circa 2 μm thickness are well-organized on millimeter scale. Like the dendritic growth of some other materials,[17] the width and thickness of dendritic crystals are mainly decided by the solubility of saturated solution and ambient temperature. It is believed that each organized dendritic crystal is grown from a single nucleus. There are at least two factors for the large-size dendritic crystal growth. At first, there is strong anisotropy in Im-ClO_4 crystals and strong low-dimensionality interaction between dendritic crystals and substrate, and thus a crystal tends to grow very fast along a preferred orientation while it grows quite slow in other orientations. Secondly, the saturated solution has a solubility of about 60%, which can allow fast crystal growth without much long-length molecular diffusion. When there was no enough area for stems and branches elongate on substrate surface and the organized dendritic crystals were formed, their stem and branches continually widened (Figure 2E) and merged to a smooth film (Figure 2F) in the Im-ClO_4 saturated solution.

The film is transparent, as seen from the optical photograph on a quartz substrate (Figure 3A). In the Im-ClO_4 film of 20×20 mm^2 in area and 2 μm in thickness, there are some different regions and each of them may be in different crystal planes. The largest region is as large as millimeter-scale (Figure 2C,D). The two most popular crystal planes are (2$\bar{1}$0) and (10$\bar{2}$), which correspond to the diffraction peak at 21.88° and 24.26° in XRD patterns, respectively. We choose the region in the (10$\bar{2}$) plane to discuss herein because the single ferroelectric polarization is along the normal direction of

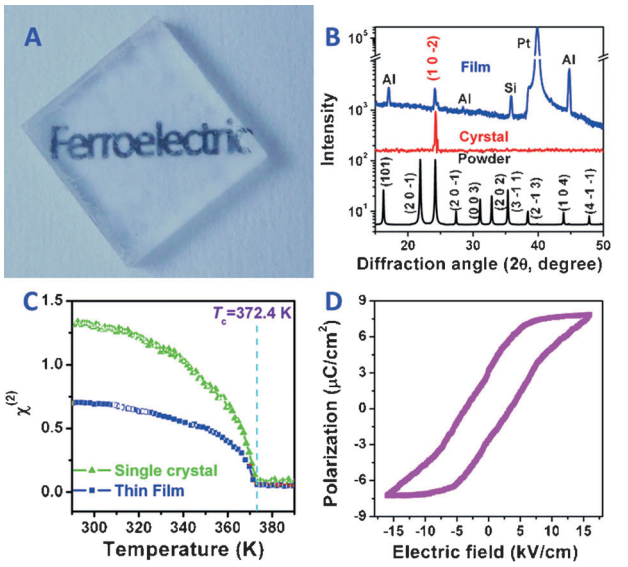

Figure 3. The film of Im-ClO_4, its orientation and properties. A) Optical photograph of the film on a quartz substrate; B) Pattern of X-ray diffraction; C) The comparison of SHG response of the film and crystals; D) Ferroelectric hysteresis loop of the film on Pt substrate.

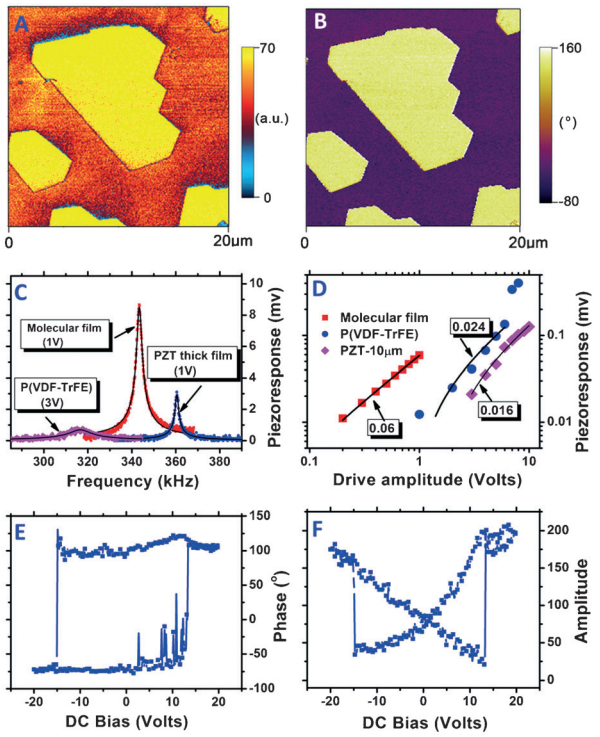

Figure 4. Piezoelectric properties of Im-ClO_4 film; A) PFM amplitude mapping; B) PFM phase mapping; C) Comparison of PFM resonance peaks of films of Im-ClO_4 (1 V), PZT (1 V), and P(VDF-TrFE) (3 V); D) Comparison of effective piezoelectric coefficient of Im-ClO_4, PZT, and P(VDF-TrFE); E) Phase–voltage hysteresis loop; and F) Amplitude–voltage butterfly loop.

(10$\bar{2}$) plane and polygonal domains can be observed (Figure 4A,B). The pattern of X-ray diffraction of this region (Figure 3B), measured from 100 μm-diameter film surface by covering other field with an aluminum foil, indicates that the film is single crystalline-like. The SHG measurement shows that the film is also polar below the transition temperature at 372.4 K (Figure 3C). This is verified by the measurement of polarization hysteresis loop, as shown in Figure 3D. The measured spontaneous polarization is as high as 7.2 μC cm^{-2}, one of the highest in molecular ferroelectric films; the coercive field is modest, only around 3.5 kV cm^{-1}. The transition of Im-ClO_4 film from ferroelectric to paraelectric phase has also been examined by PFM at a series of temperatures (Supporting Information, Figure S5). The white domain (with downward polarization) starts to shrink at 363 K, and the phase contrast disappears at 373 K, as expected from the phase transition. It is known that ferroelectric thin films may exhibit different properties from that of the bulk crystals because of surface effect and dimensional effect commonly play an important roles in $<$500 nm thin ferroelectric films. In this case, it appears that the film maintain the similar properties of the bulk crystal. This is because the film has a thickness of 2 μm and is single crystalline-like in the (10$\bar{2}$) plane. There are still strong ferroelectric properties in dendritic crystals or films with the thickness of about 200 nm. As the 1 nm-thickness $BaTiO_3$ film still shows ferroelectric properties, it is argued that ferroelectricity might be kept in 10 nm-scale Im-ClO_4 film or crystals. It is worth noting that the ferroelectricity of Im-ClO_4 has been studied before,[15] and the spontaneous polarization was found to be only around 1.0 μC cm^{-2}, which is much smaller than what we have found, despite higher polarization being predicted based on specific heat calculations. We also point out that Im-ClO_4 can be defined as an ordered–disordered ferroelectric, as can be concluded from the crystal structure and temperature-dependent physical properties. This agrees with results reported previously.[9,14d] However, it is important to emphasize that while the crystalline network of Im-ClO_4 is connected by hydrogen bonding (Supporting Information, Figure S4), there is no obvious increase of the phase-transition temperature T_c in the perdeuterated analogue D-Im-ClO_4 (Supporting Information, Figure S6), and thus the contributions of hydrogen bonds to ferroelectricity can be excluded. The structure details of D-Im-ClO_4 can be found in the Supporting Information, Figures S7–S9.

Even more interesting is the piezoelectric properties of Im-ClO_4 thin film, as we discovered from PFM. Typical PFM amplitude and phase mappings are given in Figure 4A,B, showing again the hexagonal type of domains similar to that observed in bulk crystal (Figure 1E,F). To compare the piezoresponse of Im-ClO_4 thin film with that of PZT and P(VDF-TrFE),[18] we drive each film across resonance using PFM (Figure 4C), where the strongest resonance peak is observed in Im-ClO_4 film under 1 V, which is much higher than that of PZT (1 V) and P(VDF-TrFE) (3 V), despite the fact that this PZT film shows excellent piezoelectricity.[19] It is also seen that PZT has the highest resonance frequency, while P(VDF-TrFE) has the lowest, in parallel to their relative mechanical stiffness. The resonance curves were fitted very well by the damped harmonic oscillator model,[14e] with which the quality factor can be determined, and the intrinsic piezoresponse can be derived by correcting the resonance

amplification using the quality factor. To ensure that the response is piezoelectric, such resonance measurements have been repeated under different voltages, and the intrinsic piezoresponse was plotted against the driving voltage for all three films on the log scale, which shows good linearity (Figure 4D). Again, highest slope is observed in Im-ClO_4, which is 150% higher than that of PZT, and 275% higher than that of P(VDF-TrFE), suggesting much higher effective piezoelectric coefficient in Im-ClO_4. Furthermore, switching spectroscopy PFM has been carried out on Im-ClO_4, gaving characteristic hysteresis (Figure 4E) and butterfly loop (Figure 4F), with modest coercive voltage around 15 V for film of 2 μm in thickness.

In summary, we have discovered Im-ClO_4 to be an excellent molecular ferroelectric with high spontaneous polarization and high Curie temperature, and we have successfully processed an Im-ClO_4 film that maintains its excellent ferroelectric properties, and offers superior electromechanical coupling and low coercive field, which is even better than PZT.[19,20] Our work represents a significant step for molecular ferroelectrics towards practical applications compatible to microelectronic industry, and its simple and inexpensive processing is particular advantages compared to eptaxial growth of perovskite thin films.

Experimental Section

An Im-ClO_4 (**1**) crystal of up to 0.5 cm in size was obtained by evaporation of an aqueous solution containing equal molar amounts of imidazolium chloride (200 mmol), and perchloric acid (200 mmol) at room temperature. For deuterated Im-ClO_4 (D-Im-ClO_4) (**2**) synthesis, perchloric acid (2.8 g, 20 mmol) was dissolved in D_2O (50 g). The solution was refluxed for 24 h under a N_2 atmosphere. Then, a D_2O solution of deuterated imidazolium chloride (1.44 g, 20 mmol) was added. After removing the solvent in vacuum, the resultant polycrystals were thrice recrystallized from D_2O. Single crystals of D-Im-ClO_4 were grown by slow evaporation of a D_2O solution of the resultant polycrystals at room temperature in the vacuum conditions after several days.

Single-phase Im-ClO_4 grains were dissolved in purified water to form a saturated solution with a solubility of about 60%. With this solution, 2–5 layers of thin film were deposited on $Si/SiO_2/Ti/Pt$ substrate repeatedly by the spin coating method, with the rotary speed of 3000 rev/min. After that, the film was placed in a saturated solution to induce dendrite crystal growth in the substrate plane, and a single-crystal-like thin film is formed. Finally, the grown film was annealed at 120°C for 1 hour for further measurement. The thickness of Im-ClO_4 film is about 2 mm through measurement of a man-made gap with AFM.

Differential scanning calorimetry (DSC) measurements were performed on a Perkin Elmer Diamond DSC under nitrogen atmosphere in aluminum crucibles with a heating or cooling rate of 10 K min^{-1}. For second harmonic generation (SHG) experiments, an unexpanded laser beam with low divergence (pulsed Nd:YAG at a wavelength of 1064 nm, 5 ns pulse duration, 1.6 MW peak power, 10 Hz repetition rate) was used. The instrument model is Ins 1210058, INSTEC Instruments, while the laser is Vibrant 355 II, OPOTEK. The numerical values of the nonlinear optical coefficients for SHG were determined by comparison with a KDP reference. Variable-temperature X-ray diffraction analysis was carried out on **1** and **2** using a Rigaku CCD diffractometer with Mo-Kα radiation ($\lambda = 0.71073$ Å). Data collection, cell refinement and data reduction was performed using Rigaku CrystalClear 1.3.5. The structure of **1** and **2** were solved by direct methods and refined by the full-matrix method based on F^2 using the SHELXL97 software package. All non-hydrogen atoms were refined anisotropically and the positions of all hydrogen atoms were generated geometrically. These crystal data, structure refinements, and selected geormetrical parameters can be found in the Supporting Information, Tables S1–S8. CCDC 856256, 856257, 981006, and 981007 for **1** and **2** contain the supplementary crystallographic data for this paper. These data can be obtained free of charge from The Cambridge Crystallographic Data Centre via www.ccdc.cam.ac.uk/data_request/cif.

For dielectric, ferroelectric, and pyroelectric measurements, the samples were made with single crystals cut into the form of a thin plate perpendicular to the crystal axis. Silver conduction paste deposited on the plate surfaces was used as the electrodes. Complex dielectric permittivities were measured with a TH2828A impedance analyzer over the frequency range from 500 Hz to 1 MHz with an applied electric field of 0.5 V. Dielectric hysteresis loops were recorded on a Radiant Precision Premier II. Pyroelectric property was measured with an electrometer/high resistance meter (keithley 6517B) with a heating or cooling rate of 10 K min^{-1}. The bias electric field dependence of dielectric constant was measured with an Alpha-A High performance Frequency Analyzer at 10 kHz.

PFM measurements were conducted on an atomic force microscope (Asylum Research MFP-3D and Brucker Multimode 8). On MFP-3D, a conductive cantilever with a spring constant of 2 N m^{-1} was used, and the PFM mappings were obtained under 400 mV AC voltage. To compare the PFM responses of three types of piezoelectric films, the samples were driven by different AC voltages near resonance, and the response versus frequency were fitted by the damped harmonic oscillator model (DHOM), yielding quality factors and resonant frequencies. The corrected PFM amplitudes could be calculated using PFM response (in mV) divided by quality factor. The data for PZT film under at 7 and 8 V were excluded from linear fitting of piezoelectric response versus voltage, due to prominent non-linearity possibly caused by domain switching. Furthermore, the same PFM probe was used for accurate comparison. For switching PFM, DC voltage was applied on top of the 200 mV AC voltage to switch the polarization. On Multimode 8, a conductive AFM tip (MESP-RC, Co/Cr coating, 35 nm tip Radius) was used, and an AC voltage (2 V, 41 kHz,) is used to observe phase and amplitude images. A heater is used to heat the sample with accuracy of 0.1°C.

Received: January 13, 2014
Revised: March 5, 2014
Published online: April 1, 2014

Keywords: domains · imidazolium perchlorate · molecular ferroelectrics · piezoelectric force microscopy · thin films

[1] a) H. Lu, C. W. Bark, D. Esque de Los Ojos, J. Alcala, C. B. Eom, G. Catalan, A. Gruverman, *Science* **2012**, *336*, 59–61; b) P. Maksymovych, S. Jesse, P. Yu, R. Ramesh, A. P. Baddorf, S. V. Kalinin, *Science* **2009**, *324*, 1421–1425; c) B. Neese, B. J. Chu, S.-G. Lu, Y. Wang, E. Furman, Q. M. Zhang, *Science* **2008**, *321*, 821–823; d) J. F. Scott, *Science* **2007**, *315*, 954–959.

[2] a) S. B. Lang, S. A. M. Tofail, A. L. Kholkin, M. Wojtaś, M. Gregor, A. A. Gandhi, Y. Wang, S. Bauer, M. Krause, A. Plecenik, *Sci. Rep.* **2013**, *3*, 2215–2220; b) S. H. Baek, J. Park, D. M. Kim, V. A. Aksyuk, R. R. Das, S. D. Bu, D. A. Felker, J. Lettieri, V. Vaithyanathan, S. S. N. Bharadwaja, N. Bassiri-Gharb, Y. B. Chen, H. P. Sun, C. M. Folkman, H. W. Jang, D. J. Kreft, S. K. Streiffer, R. Ramesh, X. Q. Pan, S. Trolier-McKinstry, D. G. Schlom, M. S. Rzchowski, R. H. Blick, C. B. Eom, *Science* **2011**, *334*, 958–961.

[3] a) M. Schultze, E. M. Bothschafter, A. Sommer, S. Holzner, W. Schweinberger, M. Fiess, M. Hofstetter, R. Kienberger, V. Apalkov, V. S. Yakovlev, M. I. Stockman, F. Krausz, *Nature* **2013**, *493*, 75 – 78; b) Y. L. Yu, T. Maeda, J.-I. Mamiya, T. Ikeda, *Angew. Chem.* **2007**, *119*, 899 – 901; *Angew. Chem. Int. Ed.* **2007**, *46*, 881 – 883.

[4] Y. Q. Lu, Y. Y. Zhu, Y. F. Chen, S. N. Zhu, N. B. Ming, Y. J. Feng, *Science* **2011**, *284*, 1822 – 1824.

[5] a) H. D. Megaw, *Nature* **1945**, *155*, 484 – 485; b) B. Jaffe, R. S. Roth, S. Marzullo, *J. Appl. Phys.* **1954**, *25*, 809 – 810; c) C. Y. Chao, Z. H. Ren, Y. H. Zhu, Z. Xiao, Z. Y. Liu, G. Xu, J. Q. Mai, X. Li, G. Shen, G. R. Han, *Angew. Chem.* **2012**, *124*, 9417 – 9421; *Angew. Chem. Int. Ed.* **2012**, *51*, 9283 – 9287; d) E. J. Kan, H. J. Xiang, C. H. Lee, F. Wu, J. L. Y, M.-H. Whangbo, *Angew. Chem.* **2010**, *122*, 1647 – 1650; *Angew. Chem. Int. Ed.* **2010**, *49*, 1603 – 1606.

[6] a) Z. H. Sun, T. L. Chen, J. H. Luo, M. C. Hong, *Angew. Chem.* **2012**, *124*, 3937 – 3942; *Angew. Chem. Int. Ed.* **2012**, *51*, 3871 – 3876; b) S. Horiuchi, R. Kumai, Y. Tokura, *Angew. Chem.* **2007**, *119*, 3567 – 3571; *Angew. Chem. Int. Ed.* **2007**, *46*, 3497 – 3501; c) A. Stroppa, P. Jain, P. Barone, M. Marsman, J. M. Perez-Mato, A. K. Cheetham, H. W. Kroto, S. Picozzi, *Angew. Chem.* **2011**, *123*, 5969 – 5972; *Angew. Chem. Int. Ed.* **2007**, *46*, 5847 – 5850; d) D.-W. Fu, W. Zhang, H.-L. Cai, Y. Zhang, J.-Z. Ge, R.-G. Xiong, S. D. Huang, N. Takayoshi, *Angew. Chem.* **2011**, *123*, 12153 – 12157; *Angew. Chem. Int. Ed.* **2011**, *50*, 11947 – 11951; e) G. Rogez, N. Viart, M. Drillon, *Angew. Chem.* **2010**, *122*, 1965 – 1967; *Angew. Chem. Int. Ed.* **2010**, *49*, 1921 – 11923.

[7] J. Y. Li, Y. M. Liu, Y. H. Zhang, H. L. Cai, R.-G. Xiong, *Phys. Chem. Chem. Phys.* **2013**, *15*, 20786 – 20796.

[8] S. Horiuchi, Y. Tokunaga, G. Giovannetti, S. Picozzi, H. Itoh, R. Shimano, R. Kumai, Y. Tokura, *Nature* **2010**, *463*, 789 – 792.

[9] D.-W. Fu, H.-L. Cai, Y. M. Liu, Q. Ye, W. Zhang, Y. Zhang, X.-Y. Chen, G. Giovannetti, M. Capone, J. Y. Li, R.-G. Xiong, *Science* **2013**, *339*, 425 – 428.

[10] A. S. Tayi, A. K. Shveyd, A. C.-H. Sue, J. M. Szarko, B. S. Rolczynski, D. Cao, T. JacksonKennedy, A. A. Sarjeant, C. L. Stern, W. F. Paxton, W. Wu, S. K. Dey, A. C. Fahrenbach, J. R. Guest, H. Mohseni, L. X. Chen, K. L. Wang, J. F. Stoddart, S. I. Stupp, *Nature* **2012**, *488*, 485 – 489.

[11] X.-L. Li, K. Chen, Y. Liu, Z.-X. Wang, T. W. Wang, J. L. Zuo, Y. Z. Li, Y. Wang, J. S. Zhu, J. M. Liu, Y. Song, X. Z. You, *Angew. Chem.* **2007**, *119*, 6944 – 6947; *Angew. Chem. Int. Ed.* **2007**, *46*, 6820 – 6823.

[12] J. H. Hao, Y. Zhang, X. H. Wei, *Angew. Chem.* **2011**, *123*, 7008 – 7012; *Angew. Chem. Int. Ed.* **2011**, *50*, 6876 – 6880.

[13] a) M. M. Lee, J. Teuscher, T. Miyasaka, T. N. Murakami, H. J. Snaith, *Science* **2012**, *338*, 643 – 647; b) D. J. Norris, E. S. Aydil, *Science* **2012**, *338*, 625 – 626; c) S. D. Stranks, G. E. Eperon, G. Grancini, C. Menelaou, M. J. P. Alcocer, T. Leijtens, L. M. Herz, A. Petrozza, H. J. Snaith, *Science* **2013**, *342*, 341 – 344; d) G. C. Xing, N. Mathews, S. Y. Sun, S. S. Lim, Y. M. Lam, M. Grätzel, S. Mhaisalkar, T. C. Sum, *Science* **2013**, *342*, 344 – 347; e) M. Z. Liu, M. B. Johnston, H. J. Snaith, *Nature* **2013**, *501*, 395 – 398; f) J. Burschka, N. Pellet, S.-J. Moon, R. Humphry-Baker, P. Gao, M. K. Nazeeruddin, M. Grätzel, *Nature* **2013**, *499*, 316 – 319.

[14] a) W. Zhang, R.-G. Xiong, *Chem. Rev.* **2012**, *112*, 1163 – 1195; b) H.-L. Cai, W. Zhang, J.-Z. Ge, Y. Zhang, K. Awaga, T. Nakamura, R.-G. Xiong, *Phys. Rev. Lett.* **2011**, *107*, 147601; c) D.-W. Fu, H.-L. Cai, S.-H. Li, Q. Ye, L. Zhou, W. Zhang, Y. Zhang, F. Deng, R.-G. Xiong, *Phys. Rev. Lett.* **2013**, *110*, 257601; d) D.-W. Fu, W. Zhang, H.-L. Cai, J. Z. Ge, Y. Zhang, R.-G. Xiong, *Adv. Mater.* **2011**, *23*, 5658 – 5662; e) Y. M. Liu, Y. H. Zhang, M.-J. Chow, Q. N. Chen, J. Y. Li, *Phys. Rev. Lett.* **2012**, *108*, 078103; f) Y. M. Liu, Y. J. Wang, M. J. Chow, N. Q. Chen, F. Y. Ma, Y. H. Zhang, J. Y. Li, *Phys. Rev. Lett.* **2013**, *110*, 168101.

[15] a) Z. Pająk, P. Czarnecki, B. Szafrańska, H. Małuszyńska, Z. Fojud, *J. Chem. Phys.* **2006**, *124*, 144502; b) Z. Czapla, S. Dacko, B. Kosturek, A. Waśkowska, *Phys. Status Solidi B* **2005**, *242*, R122 – R124; c) J. Przesławski, Z. Czapla, *J. Phys. Condens. Matter* **2006**, *18*, 5517 – 5524.

[16] F. Jona, G. Shirance, *Ferroelectric crystals*, Dover publications Inc, New York, **1962**.

[17] a) L. Gránásy, T. Pusztai, T. Börzsönyi, J. A. Warren, J. F. Douglas, *Nat. Mater.* **2004**, *3*, 645 – 650; b) G. L. Zhang, L. X. Jin, Z. P. Ma, X. M. Zhai, M. Yang, P. Zheng, W. Wang, G. Wegner, *J. Chem. Phys.* **2008**, *129*, 224708.

[18] Y. M. Liu, K. H. Lam, K. K. Shung, J. Y. Li, Q. F. Zhou, *J. Appl. Phys.* **2013**, *113*, 187205.

[19] K. R. Brown, C. Ospelkaus, Y. Colombe, A. C. Wilson, D. Leibfried, D. J. Wineland, *Nature* **2011**, *471*, 196 – 199.

[20] a) R. Ramesh, D. G. Schlom, *Science* **2002**, *296*, 1975 – 1976; b) J. Wang, J. B. Neaton, H. Zheng, V. Nagarajan, S. B. Ogale, B. Liu, D. Viehland, V. Vaithyanathan, D. G. Schlom, U. V. Waghmare, N. A. Spaldin, K. M. Rabe, M. Wuttig, R. Ramesh, *Science* **2003**, *299*, 1719 – 1722; c) Z. L. Wang, J. H. Song, *Science* **2006**, *312*, 242 – 246.

